Investigation of characteristic thermal signatures of breast tumors using infrared thermography

Nguyen Van Hung[1], Mai Huu Thuan[2*]

[1]Department of Radiation Physics, K3 Hospital – Tan Trieu Campus, 30 Cau Buou, Thanh Liet, Hanoi, Vietnam;
[2]Institute of Technical Physics, Hanoi University of Science and Technology, 1 Dai Co Viet, Bach Mai, Hanoi, Vietnam.
[*]Corresponding author: thuan.maihuu@hust.edu.vn
Received 12 Apr. 2026; Revised 16 Jun. 2026; Accepted 10 Aug. 2026; Published 25 Aug. 2026.
DOI: https://doi.org/10.54939/1859-1043.j.mst.113.2026.142-149

ABSTRACT

Breast cancer remains a primary cause of global cancer-related mortality, necessitating advanced early-stage diagnostic modalities. This study investigates the efficacy of infrared thermography (IRT) coupled with a systematic multi-angle acquisition protocol for characterizing malignant breast thermal signatures. A cohort of 38 patients with biopsy-proven breast cancer was evaluated using a FLUKE infrared system integrated with the BKA-06 thermal stimulation device. Thermographic data were acquired at multiple orientations (0°–180°) to comprehensively map thermal distribution patterns. Quantitative analysis identified significant thermodynamic anomalies, including elevated core temperatures, asymmetric heat dissipation, and heterogeneous isothermal contours. Recorded temperature differentials (ΔT) between tumor cores and peripheral tissues ranged from 1.2 °F to 1.8 °F. Comparative validation demonstrated high spatial congruence between thermographic "hotspots" and MRI-identified lesions, with histopathological biopsy serving as the definitive reference. Distinct from conventional binary classification approaches, this research systematically analyzes intrinsic thermal characteristics linked to pathological angiogenesis and metabolic hyperactivity. The findings suggest that the proposed IRT framework provides a reliable, non-invasive, and radiation-free adjunctive modality, enhancing the precision of early-stage breast cancer screening and clinical assessment.

Keywords: Infrared thermography; Breast cancer; Thermal imaging; Multi-angle analysis; Tumor characterization.

1. INTRODUCTION

Breast cancer remains one of the most prevalent and life-threatening malignancies among women worldwide. According to the latest estimates from the International Agency for Research on Cancer (IARC) and the World Health Organization (WHO), approximately 2.3 million new cases and nearly 670,000 deaths were reported globally in 2022 [1]. These figures account for about 11.6% of all newly diagnosed cancer cases and 6.9% of total cancer-related deaths [1]. Projections indicate that the global cancer burden will continue to rise significantly, with the number of new cases expected to exceed 35 million annually by 2050, representing a 77% increase compared to 2022 [2]. In this alarming context, early detection plays a critical role in improving prognosis and increasing patient survival rates [3]. Currently, conventional imaging modalities such as mammography, ultrasound, and magnetic resonance imaging (MRI) are widely used for breast cancer screening and diagnosis. However, these techniques present several limitations, including exposure to ionizing radiation in mammography, high operational costs, and reduced sensitivity in patients with dense breast tissue [4]. Such constraints may lead to missed lesions or delayed diagnosis, particularly in the early stages of the disease.

In recent years, infrared thermographic imaging (IRT) has emerged as a promising adjunctive modality due to its non-invasive nature, absence of ionizing radiation, and relatively low cost [5]. Recent developments in infrared detectors, thermal sensors, and uncooled microbolometers have

markedly enhanced the spatial resolution and thermal sensitivity of modern thermographic cameras, broadening their utility across military, industrial, and biomedical domains [6, 7]. In oncology, thermography has gained momentum for breast cancer detection. A 2024 systematic review demonstrated its clinical efficacy, reporting a pooled sensitivity of 88.5% [6]. To further refine diagnostic accuracy, contemporary research integrates artificial intelligence, machine learning, and FPGA-based image stitching algorithms [8, 9]. Key thermal indicators—such as vascular asymmetry, hotspot morphology, and spatial temperature heterogeneity—have proven crucial for differentiating pathological lesions from healthy tissues [8]. Moreover, recent surveys highlight the growing significance of multiscale representations, thermal texture analysis, and deep learning architectures in automating lesion classification [10].

Despite recent advances in infrared imaging technology and thermal image analysis, significant challenges remain in breast cancer thermography. Most existing studies emphasize lesion classification, whereas comprehensive investigations of intrinsic tumor thermal characteristics—including thermal gradients, heat diffusion patterns, and temperature heterogeneity—are still limited [10, 11]. Consequently, this study focuses on characterizing breast tumor thermal signatures to support non-invasive, radiation-free, and clinically feasible early-stage breast cancer detection.

2. THEORETICAL BACKGROUND AND METHODOLOGY

2.1. Physical basis of infrared thermography

Fundamental physical principles dictate that any object maintaining a temperature above absolute zero (0 K) emits electromagnetic radiation within the infrared spectrum. In medical diagnostics, the human body primarily radiates in the long-wave infrared (LWIR) band ($8 \div 14$ μm), which is quantifiable using advanced sensors [11]. The total radiant energy emitted from the skin surface follows the Stefan–Boltzmann law, where radiative power density (P) is proportional to the fourth power of absolute temperature (T), defined as $P = \varepsilon . \sigma . T^4$) [12]. Modern high-sensitivity systems, utilizing microbolometers or cooled detectors, achieve a noise equivalent temperature difference (NETD) below 30 - 50 mK, facilitating the detection of subtle cutaneous thermal variations as minute as 0.1 - 0.3 °C approx 0.18 - 0.54 °F [13]. In breast oncology, tumor progression is coupled with disrupted thermodynamic equilibrium. Malignant proliferation triggers accelerated cellular metabolism and aggressive angiogenesis, characterized by disordered microvasculature that significantly augments local blood perfusion [6]. These physiological anomalies induce localized hyperthermia and "thermal bypass" from the core to the dermal surface, manifesting as measurable temperature gradients relative to contralateral healthy tissue. Infrared thermography (IRT) captures this emission, reconstructing high-resolution 2D thermograms where "hot spots" serve as pivotal biomarkers for neoplastic activity [14].

However, IRT precision remains sensitive to multi-factorial artifacts. Accuracy is heavily influenced by environmental variables, including ambient temperature stability ($\Delta T \leq 1°C$), humidity, and convective airflow. Consequently, clinical frameworks, notably by the American Academy of Thermology (AAT), mandate rigorous acquisition protocols—including a 15–20 minute acclimatization period—to ensure the reliability and reproducibility of thermal signatures in oncological screening [15].

2.2. Instrumentation and clinical cohort

Thermal imaging data were acquired using an integrated diagnostic system comprising a BKA-06 excitation source and a FLUKE Visual IR Thermometer (USA). The BKA-06 device operates at a peak wavelength of 622.8 nm, facilitating non-invasive optical penetration into breast parenchyma with an effective depth of approximately $15 \div 17$ cm [16, 17]. To ensure metrological reliability, the excitation system was strictly calibrated in accordance with the certification standard V11.CN6.3000.23. The auxiliary infrared imaging system (FLUKE) featured a

measurement range from – 20 °C to 400 °C (– 4 °F to 752 °F) with a thermal accuracy of ± 2%. Technical specifications included a spatial resolution of 120 × 90 pixels and a spectral sensitivity range of 6.5 ÷ 14 μm, optimizing the detection of long-wave infrared (LWIR) emissions from the skin surface.

The clinical study involved a cohort of 38 patients diagnosed with breast tumors. Diagnostic confirmation for all subjects was established via histopathological biopsy—the gold standard—at K Hospital (Tan Trieu campus, n = 12) and Thai Nguyen National Hospital (n = 26). Within this cohort, a subset of 12 patients from K Hospital, recruited between September and December 2025, underwent comprehensive thermographic assessment. These specific subjects exhibited clinical manifestations of breast abnormalities and were subsequently referred for Magnetic Resonance Imaging (MRI) to correlate thermal signatures with morphological findings from clinical examinations.

Table 1. *Clinical characteristics of the breast cancer patient cohort (n = 12).*

No.	Patient's full name	Age	Tumor characteristics	No.	Patient's full name	Age	Tumor characteristics
1	Dang Thi B	47	LBT, $T_3N_1M_0$, S-IIB	7	Doan Thi D	38	RBT, $T_3N_2M_0$, S-IIIA
2	Nguyen Thi T	51	RBT, $T_3N_0M_0$, S-IIB	8	Hoang Thi H	41	LBT, $T_4N_1M_0$, S-IIIB
3	Hoang Thi T	55	LBT, $T_2N_1M_0$, S-IIB	9	Nguyen Thi Q	40	LBT, $T_4N_2M_0$, S-IIIB
4	Le Thi N	30	LBT, $T_3N_1M_0$, S-IIB	10	Pham Thi Y	58	RBT, $T_3N_2M_0$, S-IIIA
5	Le Thi H	37	RBT, $T_2N_0M_0$, S-IIA	11	Vu Thi K	48	LBT, $T_4N_2M_0$, S-IIIB
6	Ta Thi P	40	LBT, $T_2N_1M_0$, S-IIB	12	Nguyen Thị L	64	LBT, $T_4N_2M_0$, S-IIIB

Note: LBT = left breast tumor; RBT = right breast tumor; TNM = tumor–node–metastasis classification; T_1 (≤ 2 cm), T_2 (2 – 5 cm), T_3 (> 5 cm), T_4 (invasive to the chest wall or skin); N_0 Early/localized disease, N_1 Limited regional spread, N_2 Advanced regional spread; M_0 (no metastasis), S-II = Stage II; S-III = Stage III.

Patient Characteristics: A total of 12 breast cancer patients were included, all histopathologically confirmed and classified as non-metastatic (M_0). According to the TNM classification, the cohort was equally divided between Stage II and Stage III disease. Stage II cases were mainly categorized as Stage IIA–IIB, characterized by T_2–T_3 tumors with limited nodal involvement (N_0–N_1). In contrast, Stage III cases (IIIA–IIIB) were associated with locally advanced disease, including T_3N_2 and T_4 tumors with higher nodal burden. Tumor laterality analysis revealed a predominance of left breast tumors (LBT, 8/12), while right breast tumors (RBT) accounted for the remaining 4 cases.

2.3. Data acquisition protocol

Thermographic data acquisition was performed using a high-precision infrared imaging system coupled with a BKA-06 thermal excitation source. To ensure metrological integrity, measurements were conducted in a climate-controlled environment at 23 ± 1 °C (73.4 ± 1.8 °F). Participants underwent a mandatory 15-minute acclimatization period to achieve thermal equilibrium and minimize physiological variability [15]. All clinical procedures strictly adhered to institutional ethical standards, receiving formal approval from the Ethics Committee (No. 356/BVK-HDDD).

Thermographic data were acquired using a systematic multi-angle protocol across five

orientations 0° - 180° alongside vertical trajectories, centering on the tumor locus as the spatial reference. The infrared sensor was positioned perpendicularly at 0° and 180° for frontal and posterior imaging, respectively, while oblique angles (45°, 135°) captured structural and thermal heterogeneity. A 90° vertical scan evaluated the superior–inferior thermal distribution. This multi-directional approach enabled precise mapping of heat diffusion gradients within the tumor microenvironment, ensuring a high-fidelity representation of pathological thermodynamic behavior.

Figure 1. *Thermographic data acquisition protocol: (a) Schematic representation of imaging orientations; (b) Operational procedure for thermal capture; (c) Clinical imaging implementation; (d) Spatial data acquisition of thermal points surrounding the anomalous region.*

2.4. Image processing and thermal feature extraction

The proposed experimental workflow comprised three sequential phases: thermographic pre-processing, quantitative feature extraction, and clinical validation. Initially, Regions of Interest (ROIs) were segmented based on anatomical landmarks to maintain spatial consistency. Raw thermograms were normalized and contrast-enhanced utilizing integrated software tools on the FLUKE system to mitigate environmental noise and isolate pathological hyperthermia.

The core boundary was defined by a relative threshold criterion: $T_{hotspot} \geq T_{background} + 1.2\ ^{o}F$. A multidimensional set of thermal descriptors was extracted to quantify tissue thermodynamics. Key parameters included statistical metrics—peak (Tmax), nadir Tmin), and mean temperatures—alongside thermal heterogeneity, which measures spatial variance and gradient distributions as indicators of metabolic hyperactivity. Furthermore, morphological and chrominance analyses assessed "hot spot" geometry and pseudo-color distribution to identify focal hyperthermia associated with potential malignancy.

Finally, clinical validation was established by benchmarking these spatial differentials against structural MRI and histopathological biopsies. Crucially, image interpretation was conducted by blinded evaluators independent of clinical records. This comparative framework enabled a rigorous assessment of tumor localization and staging, confirming that functional thermodynamic signatures correspond directly to the underlying metabolic and angiogenic status of the lesion

3. RESULTS AND DISCUSSION

3.1. Thermographic imaging results in patients

Representative patient thermograms acquired at multiple viewing angles illustrate spatial variation in thermal patterns across different perspectives. Analysis of intensity and color distribution, reflecting surface temperature variations, reveals a distinct boundary between suspicious lesions and surrounding healthy tissue (Figure 2). As depicted in images (a–f), the central region of the suspected lesion displays intense deep red tones, corresponding to an elevated temperature of approximately 93.4 °F. In contrast, adjacent areas exhibit lighter hues with lower temperatures around 90.2 °F, establishing a pronounced thermal gradient between the lesion core and surrounding parenchyma. This core-to-periphery gradient reflects underlying pathophysiological alterations within malignant tissue. Elevated core temperatures correlate with

high cellular density, local hypermetabolism, and angiogenesis-induced vascularization, which accelerate regional blood perfusion and heat dissipation. Conversely, non-pathological parenchyma demonstrates a lower, homogeneous thermal baseline. The micro-spatial thermal variations detected within the lesion further reflect structural and functional heterogeneity, serving as critical biophysical indicators for anomalous tissue identification and characterization.

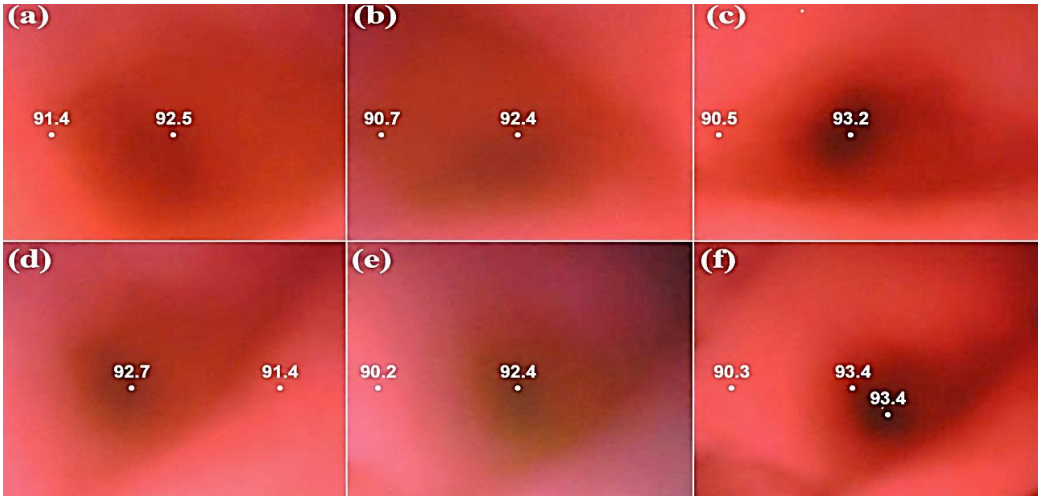

Figure 2. *Thermal images of the breast tumor in patient Dang Thi B acquired at different viewing angles: (a) 0°, (b) 45°, (c) 90°, (d) 135°, (e) 180°, and (f) top view.*

Following segmentation of the region of interest (ROI) and temperature normalization, thermal features were extracted along profiles passing through the lesion center. Representative results are illustrated in Figure 3.

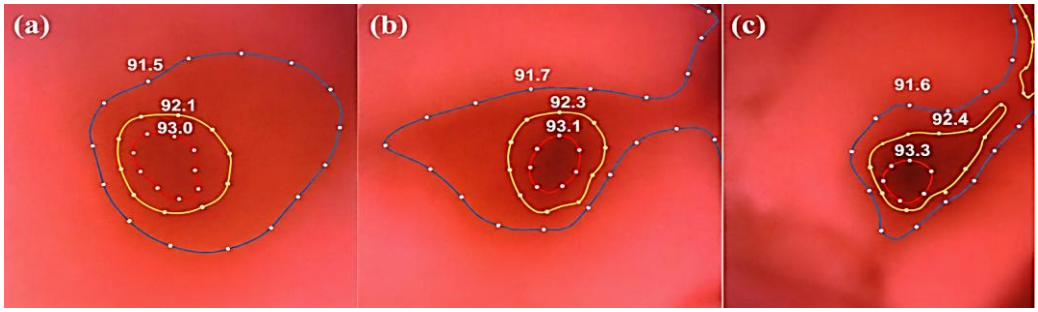

Figure 3. *Spatial data acquisition of thermal points surrounding anomalous regions across clinical subjects: (a) Patient Doan Thi D; (b) Patient Vu Thi K; and (c) Patient Dang Thi B.*

Thermographic Signature Analysis: Figure 1 displays representative breast thermograms exhibiting pathognomonic thermal signatures of underlying malignancy. Quantitative analysis reveals distinct isothermal contours defining dynamic temperature gradients. A pronounced hyperthermic core (red isotherms) is identified with peak temperatures of 93.0 °F – 93.3 °F, characterized by steep gradients relative to the periphery. The intermediate zone (yellow isotherms) ranges from 92.1 °F – 92.4 °F, while the outer boundary (blue isotherms) registers approximately 91.5 °F – 91.7 °F.

The core-to-periphery temperature differential (ΔT) approximates 1.2 °F to 1.8 °F. In clinical IRT protocols, gradients exceeding 1.0 °C (approx 1.8 °F) provide significant diagnostic evidence for tumor angiogenesis and altered metabolic heat production [6]. Morphologically, Figure. 1a demonstrates focal, concentric contours suggesting a localized lesion. Conversely, Figure. 1b and 1c exhibit increasing morphological asymmetry and expanded thermal diffusion patterns. This observed

thermal heterogeneity and irregular contour morphology are critical biomarkers, correlating with the chaotic microvasculature and metabolic demand typical of high-grade neoplasms [14].

3.2. Comparative diagnostic validation

To evaluate the diagnostic efficacy of infrared thermography (IRT), identified hyperthermic regions were systematically cross-referenced with Magnetic Resonance Imaging (MRI) datasets, the latter serving as a high-fidelity reference for morphological staging. Figure 4 illustrates representative findings from the clinical cohort, demonstrating the spatial correlation between thermal anomalies and structural pathology.

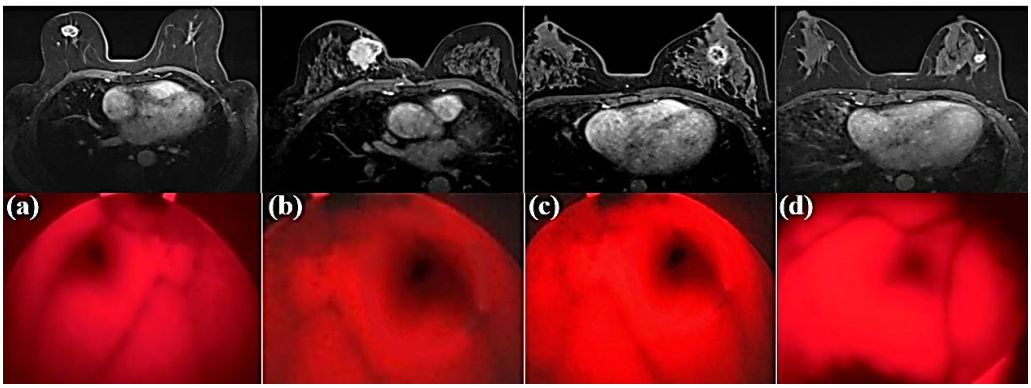

Figure 4. *Comparative MRI and infrared thermographic (IRT) scans of selected patients: (a) Hoang Thi T; (b) Vu Thi K; (c) Pham Thi Y; (d) Le Thi H.*

Figure 4 demonstrates high spatial congruence regarding tumor localization, dimensions, and morphology. MRI findings reveal neoplastic lesions characterized by high signal intensity, irregular margins, and stromal infiltration, predominantly within the upper-outer quadrant (UOQ). Correspondingly, IRT identifies "thermal cores" spatially synchronized with these malignant masses, validating the system's localization precision.

Thermal radiation patterns in Figures (a–c) serve as pathognomonic indicators of angiogenesis, where neo-vascularization facilitates enhanced heat transfer from deep-seated tumors to the cutaneous surface. In contrast, the lesion in MRI image (d) is situated deeper than those in (a–c), resulting in a less intense thermal core due to increased tissue attenuation. Quantitative analysis indicates that larger, invasive masses identified via MRI consistently manifest as more expansive thermographic signatures.

While MRI, CT, and IRT are effective for detecting physiological and structural anomalies, their findings must be cross-validated. Histopathological biopsy remains the definitive gold chuẩn for differentiating between benign and malignant pathologies and confirming the underlying biological status of the identified lesions.

3.3. Comparative validation with histopathological biopsy results (n = 26)

The clinical study comprised a cohort of 26 female patients (age range: 34–70 years) admitted to the Oncology Department at Thai Nguyen Central Hospital. All participants had previously undergone clinical examinations and received a definitive diagnosis of breast cancer via histopathological biopsy. The comprehensive data regarding their thermographic characteristics and pathological profiles are summarized in Table 2.

The consolidated results presented in Table 2, comprising 26 biopsy-confirmed breast cancer patients, provide a representative dataset for evaluating the capability of the proposed infrared thermography (IRT) system. Invasive ductal carcinoma (NST) constituted the predominant histopathological subtype, accounting for 84.6% of the cohort. All examined malignant cases exhibited measurable thermal abnormalities, characterized by localized hyperthermia at the lesion

site following BKA-06 excitation. Most tumors presented a temperature difference (ΔT) of ≥ 1.2 °F relative to the surrounding tissue, indicating increased metabolic activity associated with malignant progression. More advanced lesions (Stage II–III) generally demonstrated higher thermal intensity and more pronounced hotspot formation than early-stage tumors.

Table 2. *Summary of Clinicopathological Data and Thermographic Features (n=26).*

Parameter	Category	Value / distribution	Associated thermographic abnormalities (IRT)
Total cohort	Sample size	n = 26	Thermal Gradient (ΔT): Pathological elevation ranging from 1.2 °F to 1.8 °F compared to contralateral baseline.
Demographics	Age range	34 - 70	Nodal involvement: Extended thermal dissipation towards the axillary region in metastatic cases.
Histopathology	Invasive carcinoma	22/26 (84.6%)	Core Characteristics: Prominent "hotspots" exhibiting bright red or white-scale intensity at the tumor locus.
	Metastatic carcinoma	4/26 (15.4%)	Vascular Signatures: Asymmetric peri-tumoral hyperthermia indicative of pathological angiogenesis.
Histologic grade	Stage II & III	8/26 (30.8%)	Metabolic Intensity: High-grade tumors correlated with steeper thermal gradients and irregular isothermal contours

The spatial correspondence between biopsy-confirmed lesions and thermographically detected hotspots suggests that infrared imaging is capable of capturing functional physiological alterations associated with tumor angiogenesis and elevated blood perfusion. Furthermore, the multi-angle acquisition protocol (0°–180°) enabled comprehensive visualization of temperature distribution, improving the assessment of thermal gradients and heterogeneous heat patterns compared with single-view imaging. Combined with the FLUKE thermal camera, the BKA-06 imaging platform provides a non-invasive, radiation-free, and cost-effective approach for characterizing breast tumor thermal signatures. Although infrared thermography cannot replace conventional imaging or histopathological examination, it demonstrates considerable potential as an adjunctive technique for improving early breast cancer screening and functional assessment

4. CONCLUSIONS

Based on the principles of infrared thermodynamics and a systematic multi-angle data acquisition approach, this study investigated the thermal signatures of breast tumors in a cohort of 38 patients. Using the BKA-06 stimulation source combined with the FLUKE thermographic measurement system, characteristic thermal biomarkers, including elevated core temperature and asymmetric heat dissipation, were identified and validated against histopathological biopsy as the gold-standard reference. The novelty of this work lies in the systematic evaluation of intrinsic thermal features, such as thermal gradients and isothermal contour distributions, rather than relying solely on conventional binary classification approaches. The obtained results demonstrated high spatial agreement between infrared thermography (IRT) “hotspots” and MRI findings, indicating comparable localization capability to established structural imaging standards. These findings highlight the potential application of the proposed method as a screening examination, non-invasive, cost-effective adjunct tool for early-stage breast cancer screening and clinical diagnosis.

Acknowledgement: *This research was funded by the basic research project BENH VIEN K, number: 1002/QD-BVK-131.*

REFERENCES

[1]. F. Bray et al., “*Global cancer statistics 2022: GLOBOCAN estimates of incidence and mortality worldwide for 36 cancers in 185 countries*”, CA: A Cancer Journal for Clinicians, Vol. 74, No. 3, pp. 229–263, (2024).

[2]. International Agency for Research on Cancer (IARC), "*Global cancer burden growing, amidst mounting need for services*", World Health Organization News, (2024).
[3]. R. A. Smith et al., "*Cancer screening in the United States, 2024: A review of current American Cancer Society guidelines and current issues in cancer screening*", CA: A Cancer Journal for Clinicians, Vol. 74, No. 2, pp. 121–149, (2024).
[4]. K. Kerlikowske et al., "*Proportion of women with dense breasts at high risk for screening-detected and interval cancer: A cohort study*", Annals of Internal Medicine, Vol. 176, No. 2, pp. 151–160, (2023).
[5]. B. B. Lahiri, S. Bagavathiappan, T. Jayakumar and J. Philip, "*Medical applications of infrared thermography: A review*", Infrared Physics & Technology, Vol. 55, No. 4, pp. 221–235, (2012).
[6]. T. Nguyen et al., "*Diagnostic efficacy of modern infrared thermography for breast cancer: A systematic review and meta-analysis of studies from 2010 to 2024*", Medical Physics, Vol. 51, No. 4, pp. 2845–2860, (2024).
[7]. T. D. Nguyen et al., "*Advances in thermal imaging technology for military applications*", Journal of Military Science and Technology, No. 89, pp. 173–176, (2023).
[8]. L. F. Silva et al., "*Machine learning-based feature extraction and classification of breast thermograms: A comparative study*", Computers in Biology and Medicine, Vol. 154, p. 106560, (2023).
[9]. H. N. Quang, T. D. Hoa and D. Van Tang, "*Image fusion using FPGA in multi-sensor optoelectronic systems*", Journal of Military Science and Technology, Vol. 104, pp. 130–136, (2025).
[10]. Y. Zhang et al., "*Survey on thermal texture analysis, multiscale representation, and deep learning in breast lesion classification*", Expert Systems with Applications, Vol. 215, p. 119210, (2025).
[11]. B. B. Lahiri, "*Infrared thermography in clinical practice: A literature review of theoretical foundations and applications*", Journal of Thermal Biology, Vol. 128, p. 103892, (2025).
[12]. J. R. Howell, M. P. Mengüç and K. Daun, "*Thermal Radiation Heat Transfer*", 7th ed., CRC Press, New York, NY, USA, (2023).
[13]. X. Wang, J. Liu and R. Zhang, "*High-resolution IR image stitching and real-time processing using FPGA for clinical diagnostics*", IEEE Access, Vol. 12, pp. 45120–45135, (2024).
[14]. S. Hosseini et al., "*Using independent components analysis and AI to identify breast cancer thermal signatures*", IEEE Transactions on Medical Imaging, Vol. 43, No. 1, pp. 112–125, (2026).
[15]. American Academy of Thermology (AAT), "*Guidelines for breast thermography and medical infrared imaging*", AAT Clinical Standards, (2024).
[16]. H. T. Mai, D. Q. Ngo, H. P. T. Nguyen and D. D. La, "*Fabrication of a reflective optical imaging device for early detection of breast cancer*", Bioengineering, Vol. 10, No. 11, p. 1272, (2023).
[17]. M. H. Thuan et al., "*Development of a vein detection device based on energy spectrum method combined with infrared thermal imaging*", Journal of Military Science and Technology, No. 88, pp. 115–122, (2023).

TÓM TẮT

Nghiên cứu các dấu hiệu nhiệt đặc trưng của khối u vú bằng phương pháp ảnh nhiệt

Ung thư vú hiện là nguyên nhân gây tử vong hàng đầu ở phụ nữ toàn cầu, đặt ra yêu cầu cấp thiết về các phương pháp chẩn đoán sớm. Nghiên cứu này đánh giá hiệu quả của phương pháp đo nhiệt hồng ngoại (IRT) kết hợp kỹ thuật thu thập dữ liệu đa góc để nhận diện các dấu hiệu nhiệt đặc trưng của khối u. Thực nghiệm được tiến hành trên 38 bệnh nhân (đã xác chẩn bằng mô bệnh học), bằng hệ thống hồng ngoại FLUKE phối hợp thiết bị gia nhiệt BKA-06. Dữ liệu nhiệt được thu nhận tại nhiều góc độ (0°–180°) để lập bản đồ phân bố nhiệt một cách toàn diện. Kết quả phân tích định lượng tại vùng ác tính cho thấy các bất thường rõ rệt: nhiệt độ vùng lõi tăng cao, phân bố nhiệt mất đối xứng, độ dốc nhiệt lớn và đường đẳng nhiệt không đồng nhất. Chênh lệch nhiệt độ (ΔT) giữa vùng lõi khối u và mô lân cận dao động trong khoảng 1.2 °F to 1.8 °F. Đáng chú ý, các "điểm nóng" trên ảnh nhiệt có sự tương đồng cao về không gian với tổn thương trên MRI. Khác với các tiếp cận phân loại nhị phân thông thường, nghiên cứu này tập trung phân tích sâu đặc tính nhiệt liên quan đến sinh lý khối u và sự tăng sinh mạch máu. Kết quả khẳng định IRT là phương pháp bổ trợ không xâm lấn, không bức xạ và tối ưu chi phí trong sàng lọc ung thư vú sớm.

Từ khoá: Đo nhiệt hồng ngoại; Ung thư vú; Hình ảnh nhiệt; Phân tích đa góc; Đặc điểm hóa khối u.